

# Analysis of the Relationship between Load and EEG by Wavelet Transform for BMI

Kazuhiro Uemto, Masataka Yoshioka, Yuichiro Yoshikawa, and Chi Zhu

Maebashi Institute of Technology,  
460-1, Kamisadorimachi, Maebashi-shi, Gumma, 371-0816, Japan  
{m1356001,zhu}@maebashi-it.ac.jp

**Abstract.** Recently, a variety of researches and developments on BMIs attract many researchers' attentions. However, most of these BMI researches intend to assist the disabled. The purpose of this study is the development of real-time power assist technology using BMI that can also be used even for healthy people. To achieve this we consider that motion identification by EEG is necessary. In this paper, we analyzed the experimental data and tried to clarify the relationship between EEG and load by wavelet transform. From our results, some interesting characteristics are obtained. It shows the possibility to extract the motion information from EEG.

**Keywords:** EEG, Load, Wavelet Transform, Brain-Machine Interface.

## 1 Introduction

Currently, Japan has entered the aging society and it is estimated that the population over the age of 65 will be more than 40 percent in 2030. Continuously increasing of the old people needing to be cared and consequently increasing of the caregivers' burden become very serious society problems. Therefore, development of medical and assistive devices is an urgent need in order to solve such problems. Recently, development of the devices using human biological signals has received a lot of attentions. For example, many power assist devices have been being developed with EMG to support the persons whose muscle has declined and to reduce the burden of caregivers.

Because of aging or severely disorder, some people lost their motion ability or communication ability. To help them, recently, BMI (Brain-Machine Interface) that can operate external machines with only brain activity has been attracting attention and is expected to introduce to the field of the medical and nursing cares [1–3].

Invasive BMI, in which electrodes are directly inserted into human or animal brain is pioneered by John K. Chapin and Miguel A. L. Nicolelis [4]. In their study, the rat who was inserted electrodes into the motor cortex of the brain was trained to be able to control a robot arm by the activity of motor cortex. Then, they conducted research using monkeys. As with rats, monkeys who embedded electrodes into the primary motor cortex could operate a joystick to the left

or right side corresponding to the lighting of the lamp on the left and right of the screen in front of the him. Further, the robot arm was controlled to realize the different tasks according to the neuron activities in the motor cortex [5]. Moreover, recently, study results have been reported with human subjects, in which, patients who are inserted electrodes into the brain, were able to grasp a bottle for water drinking by controlling the robot arm with their movement intention [6]. It is also reported that it is possible to realize more accurate motions by repeated training with their BMI technology. Invasive BMI requires recording electrodes implanted in the cortex and function well for long periods, and they risk infection and other damages to the brain.

On the other hand, non-invasive BMIs for human users derive the user's intent from scalp-recorded EEG (electroencephalogram) activity. Because these systems do not require invasive surgical implants, they can be used for wide range of applications. For example, the wheelchair was successfully controlled by interpreting the intention from EEG of the operator. A EEG keyboard was developed by the visual information from EEG of the operator [7, 8]

But, up to today, the emphases of these studies are mainly to support the disabled person. In other words, BMI are not yet developed to reconcile the healthy persons and the disabilities persons. Therefore, our research focuses on the development of a novel power assist technology, that can be used for both the healthy persons and disabilities persons.

For this purpose, it is essential to examine the characteristics of the human EEG. Current, a variety of EEG have been founded. For example, Slow Cortical Potential(SCP), Event Related Potential(ERP), Steady State Visually Evoked Potential(SSVEP), Sensorimotor Rhythms(SMR) and so on [9–11]

Further, the coherence between muscle and brain has been investigated in isometric exercise that does not change the length of the muscle in the study on communication between the brain and muscle [12]. This study investigated the coherence between EEG and EMG during extension and flexion of forearm. It is found that there exists coherence during extension in the beta frequency band(15-30[Hz]).

However, up so far, there are still not a clear report about the relationship between EEG and payload. Therefore, clarifying the relationship is considered to be very beneficial in helping to develop a novel power assist technology by BMI. In this paper, we conduct experiments and analyze the EEG signals in order to clarify the relationship between EEG and payload. Since scalogram is the square of the wavelet coefficients, it implies the power of each frequency band. In this paper, we compare the changes of the scalogram of  $\alpha$  and  $\beta$  rhythms in in-motion with the changes in pre-motion by wavelet transform, and investigate the tend of the changes with respect to four different payloads.

## 2 EEG Analysis Using Wavelet Transform

Processing in the BMI is shown Table.1. In feature extraction, we use Wavelet transform. Wavelet transform uses a small wave called mother wavelet as

**Table 1.** List of processing in the BMI

Measuring	International 10-20 system
Preprocessing	EEG
Feature extraction	$\alpha, \beta$ rhythm
Distinction	Transition rate of $\alpha, \beta$ rhythm

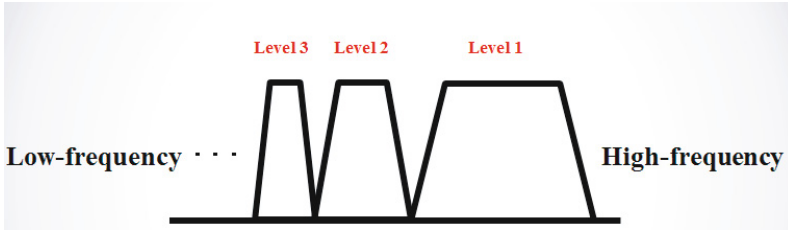


**Fig. 1.** Schematic diagram of multi-resolution analysis

reference while it stretches to a variety of scales and moves along time axis to analyze the signals. Therefore, wavelet transform can realize simultaneous time-frequency transformation. It has better time-frequency resolutions than the FFT and STFT (short time fourier transform) are well used in conventional signal processing. In this study, we use wavelet transform to analyze the EEG signals.

**2.1 Wavelet Transform and Multi-resolution Analysis**

Wavelet transform is basically cataloged into two kinds, Continuous Wavelet Transform (CWT) and Discrete Wavelet Transform (DWT). CWT is mainly used to analyze patterns in the data and their similarity. It is suitable for accurate analysis but its processing speed is slow. On the other hand, DWT is used to energetic analysis and data compression. Its analysis result is inferior to CWT, but its processing speed is fast. Therefore, in this study we use Multi-Resolution Analysis (MRA)(Fig.1) of DWT to process EEG signals [13–15]In MRA, the signal is divided into two parts by a LPF and a HPF. Repeated this process, decomposition of the signal to each frequency band can be performed. In other words, DWT can extract the specific frequency band [16].

**2.2 EEG Analysis by MRA**

In this study, we calculate the wavelet coefficients corresponding to the  $\alpha$  and  $\beta$  frequency bands in EEG signals with MRA. Assume signal data are  $x_n$ , wavelet coefficients can be calculated

$$W_l = \frac{1}{\sqrt{2^{L-l}}} \sum_n x_n \psi\left(\frac{t - k2^{L-l}}{2^{L-l}}\right) = \frac{1}{\sqrt{2^{L-l}}} \sum_n x_n \psi\left(\frac{t}{2^{L-l}} - k\right) \quad (1)$$

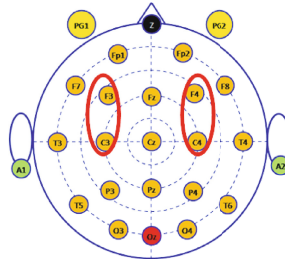


**Fig. 2.** International 10-20 system . Red circle represent the measuring points in this experiment.

Where,  $2^{L-l}$  and  $k2^{L-l}$  are variable which obtained by dividing the binary shift time and scale of the mother wavelet; function  $\phi$  is wavelat function;  $L$  is positive integer which shows thr level of signals;  $l$  is variable which represents the level of MRA;  $n$  is number of data;  $k$  is variable which represents range of shift time .  $W_l$  is wavelet coefficient. Frequency band becomes narrower octave interval with level  $l$  becomes  $(L - 1)$ ,  $(L - 2)$ ,  $(L - 3)$ .. The square of the wavelet coefficients note that is called scalogram. It implies the power of each frequency band.

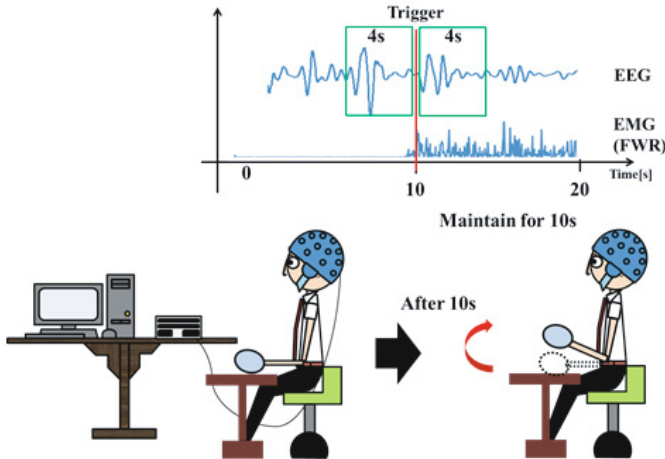


**Fig. 3.** Schematic diagram of experiment

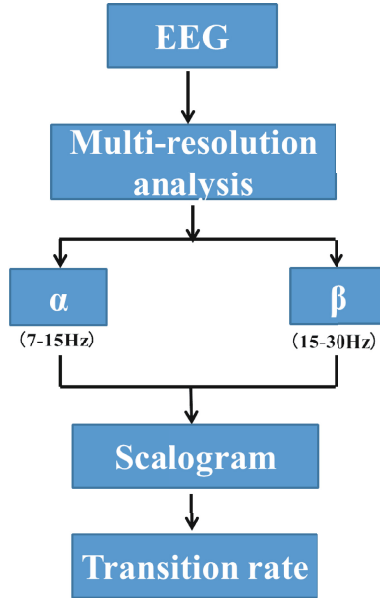


Fig. 4. Processing method

### 3 Relationship Extraction between EEG and Motor by Wavelet Transform

This section discusses the processing methods of EEG data measured in pre-motion and in-motion by MRA and calculates the transition rate of each frequency band at measuring points  $C_4$  and  $F_4$ .

#### 3.1 Experimental Design

In experiments, four different payloads 1, 3, 5, 7[kg] are used. In fact, these payloads are four different dumbbells. Measuring points are  $C_4$  and  $F_4$  near the motor cortex according to international 10-20 system (Fig.2). The subject is sitting in a chair and holding payload (dumbbell) with his left hand. The payload is put on the table in advance and the subject is in rest state at the beginning as shown in left figure in Fig.3. Then the measurement is started. After about 10 seconds, the subject holds up his arm and lifts off the payload from the table for 10 seconds. Meanwhile the EMG (electromyography) at biceps brachii is also measured. In these experiments, the rise of the EMG is used as an indicator to detect the time instant of holding up. The EEG data before and after 4 seconds of holding up (i.e. at the EMG rising instant) are extracted. In this paper, the states before and after holding up are called as pre-motion and in-motion, respectively. The experiments are implemented with total four subjects.

### 3.2 Analysis Method

We perform MRA to the EEG data respectively for four payloads 1, 3, 5, 7[kg] (Fig.4). Then we calculate the scalogram of each frequency band. Further, we calculate the average of each scalogram of data in pre-motion and in-motion around the EMG indicator. Finally, we calculate the transition rate in in-motion with respect to the pre-motion, and investigate the transition of each EEG frequency band at the measuring points. The transition rate is expressed as

$$TR = \frac{IM - PM}{PM} \times 100 \quad (2)$$

[TR: Transition Rate, IM: The scalogram in in-motion, PM: The scalogram in pre-motion]

If the transition rate is positive, it means that scalogram of in-motion increases with respect to the scalogram in pre-motion. If transition rate is negative, it implies the scalogram of in-motion is lesser than the one pre-motion. The analysis procedure is shown in Fig.4.

## 4 Analysis Results

In this section, we discuss the experimental results at the contralateral points  $F_4$  and  $C_4$  with four subjects.

Analysis results of  $\alpha$  rhythm at points  $F_4$  are shown in Fig.5. For subject A, his transition rates are negative. It means that the scalogram of  $\alpha$  wave in in-motion decreases with respect to the pre-motion. Moreover, the transition rate becomes higher in the negative direction as the weight becomes heavier. This shows that the scalogram of  $\alpha$  wave in in-motion decreases with the increasing of the payloads. For subject B, his transition rate is totally decreases with the increasing of the payloads, though the transition rate of 5[kg] is bigger than the rate of 3[kg]. For subject C, similar to the result for subject B, the negative transition rate of 7[kg] is bigger than the rate of 5[kg], but the transition rate basically higher in the negative direction for all of payloads. For subject D, different from the other three subjects, his transition rate increases with the payloads. But, note that his transition rates of all payloads are still negative.

Analysis results of  $\alpha$  rhythm at  $C_4$  are shown in Fig.6. For subject A, his transition rates are negative at 3, 5, 7[kg], but positive at 1[kg]. It shows that the transition rates are not always positive or negative for all of payloads. For subject B, his transition rates are negative at 1, 7[kg], but positive at 3, 5[kg]. It also shows that the transition rates are not always positive or negative for all of payload. For subject C, very similar to his transition rate trend at  $F_4$ , his transition rates at  $C_4$  basically decrease with the increasing of the payloads, though the rate at 7[kg] is slightly bigger than the one at 5[kg]. For subject D, his transition rates are negative at 1, 7[kg], but positive at 3, 5[kg]. It also shows that the transition rates are not always positive or negative for all of payloads.

Analysis results of  $\beta$  rhythm at  $F_4$  are shown in Fig.7. For subject A, his transition rates are negative at 1, 3[kg], but positive at 5, 7[kg]. It shows that the

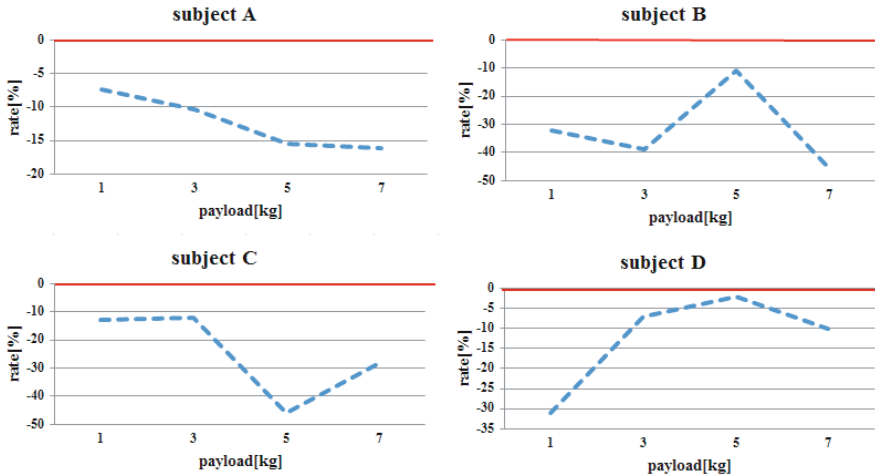


**Fig. 5.** Analysis result of  $\alpha$  rhythm at  $F_4$ . Solid line represent that transition rate is 0. (Up left and right is subject A, B. Lower left and right is subject C, D.)

transition rates are not always positive or negative for all of payloads. For subject B, his transition rates decrease with the increasing of the payloads, though the rate at 5[kg] is slightly bigger than the one at 3[kg]. For subject C, his transition rates are positive, and the rates increases with the increasing of the payloads, though the rate at 5[kg] is slightly lower than the one at 3[kg]. It means that the scalogram of  $\alpha$  wave in in-motion state increases with respect to the pre-motion. For subject D, his transition rates generally decreases with the increasing of the payloads, though the rate at 7[kg] is slightly bigger than the one at 5[kg].

Analysis results of  $\beta$  rhythm at  $C_4$  are shown in Fig8. For subject A, his transition rates nearly decrease with the increasing of the payloads, though the rate at 7[kg] is slightly bigger than the one at 5[kg]. For subject B, very similar to his transition rates trend at  $F_4$ , his transition rates at  $C_4$  basically decreases with the increasing of the payloads, though the rate at 5[kg] is bigger than the one at 3[kg]. For subject C, his transition rates at 1, 3, 5[kg] almost do not have change, but they are positive for all of payloads. For subject D, the transition rate are negative at 1, 5[kg], and positive at 3, 7[kg]. It means that the transition rates are not always positive or negative for all of payloads.

## 5 Conclusion and Future Works

### 5.1 Conclusion and Remarks

Now we summarize the analysis results of  $\alpha$  rhythm for the four subjects. First of all, we can find from Fig.5 and Fig.6 that the transition rate of each subject has the almost same trend with respect to the payloads. For subject A, B, C,

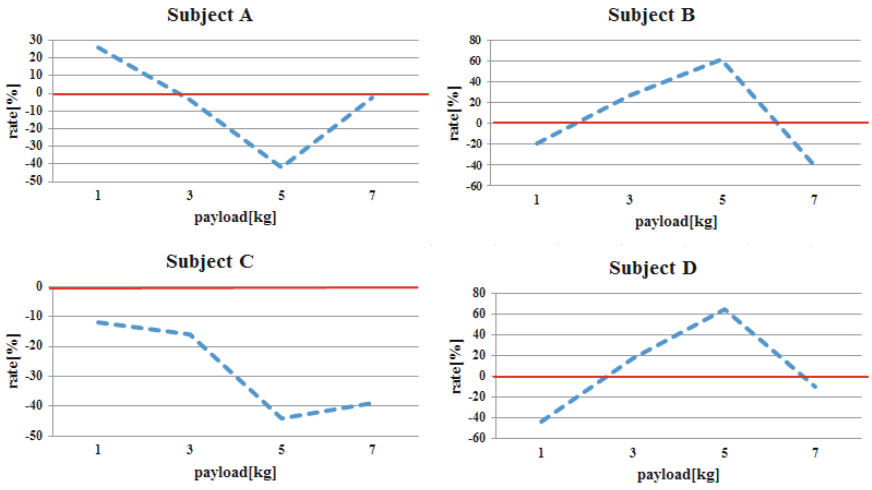


**Fig. 6.** Analysis result of  $\alpha$  rhythm at  $C_4$ . Solid line represent that transition rate is 0. (Up left and right is subject A, B. Lower left and right is subject C, D.)

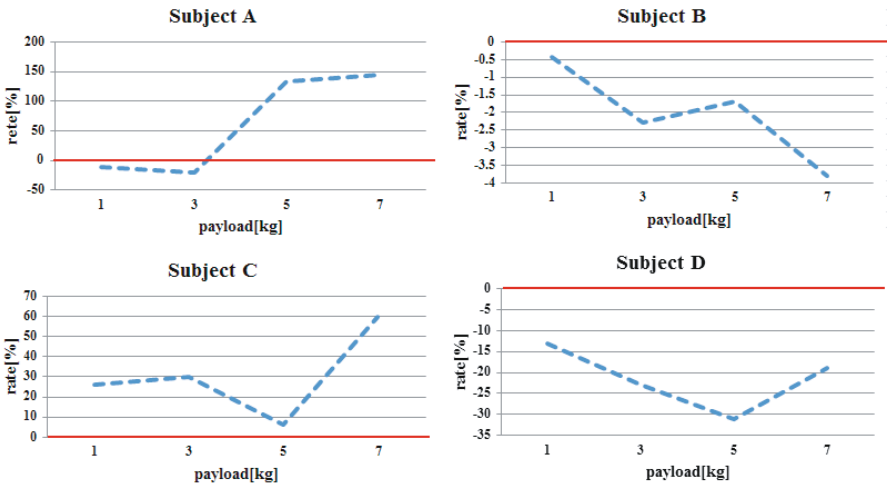


**Fig. 7.** Analysis result of  $\beta$  rhythm at  $F_4$ . Solid line represent that transition rate is 0. (Up left and right is subject A, B. Lower left and right is subject C, D.)



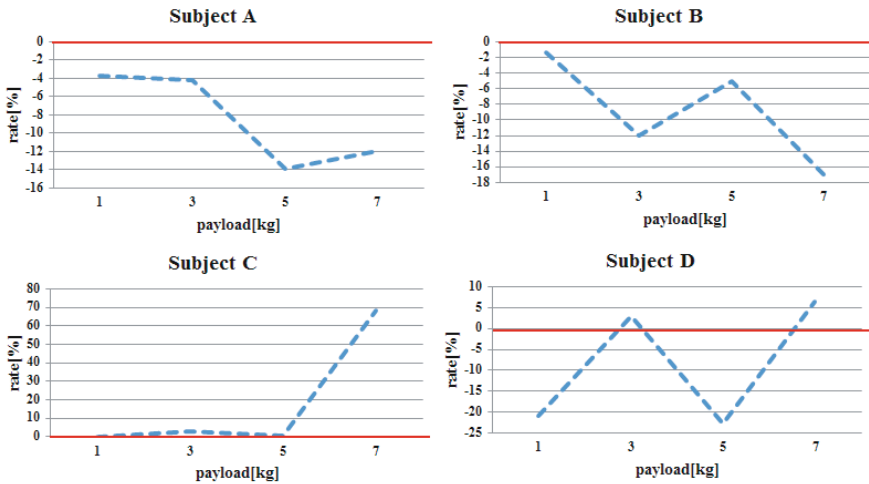


**Fig. 8.** Analysis result of  $\beta$  rhythm at  $C_4$ . Solid line represent that transition rate is 0. (Up left and right is subject A, B. Lower left and right is subject C, D.)

their transition rates are generally decrease with the increasing of payloads. It coincides with the well known fact that  $\alpha$  rhythm (or saying,  $\mu$  rhythm, 8-12Hz) is suppressed in motor imaginary or motion. Here, we further make it clear that the  $\alpha$  rhythm may be suppressed by the loads, not only by the motion imaginary and / or motion. But, subject D's transition rate takes different property. It almost increases with the payloads. Therefore, it is one of our future works to further intensively investigate the cause. On the other hand, with regard to the results of  $\beta$  rhythm for all four subjects, we can find that the transition rates of subject B and subject C respectively have the almost same trend about the payloads, in which, the transition rates of subject B generally decrease with the loads while the transition rates of subject C roughly increase with the loads. But the transition rates of subject A at  $F_4$  and  $C_4$  take opposite trends about the loads. For subject D, his transition rates do not have a obvious trend about the load (Fig.7, 8). These results show that the  $\beta$  rhythm is greatly dependent on the individuals and it is not easy to get the relationship between the  $\beta$  rhythm and the payloads. This is probably because  $\beta$  rhythm consists of two parts, i. e. some  $\beta$  rhythms are harmonics of  $\alpha$  ( $\mu$ ) rhythms and some an independent of the  $\alpha$  ( $\mu$ ) rhythms. Therefore, it would be necessary to differentiate the two parts of  $\beta$  rhythms and investigate the trend of the independent part about the load.

## 5.2 Future Works

In this paper, we investigate the relationship between EEG and the payloads with wavelet transform. It is found that the  $\alpha$  rhythm basically decrease with the payloads and  $\beta$  rhythm is greatly dependent on the individuals.

As a future work, we will increase the subjects to obtain more data to clarify the cause of the different trends between the measurement points and the subjects. Meanwhile, we will redesign the experiments to further investigate the relationship between EEG and loads.

## References

1. Birbaumer, N., Cohen, L.G.: Brain-computer interface: communication and restoration of movement in paralysis. *J. Physiol.* 579(3), 621–636 (2007)
2. Wolpaw, J.R., Birbaumer, N., McFarland, D.J., Pfurtscheller, G., Vaughan, T.M.: Brain-computer interfaces for communication and control. *Clinical Neurophysiology* 113, 767–791 (2002)
3. Sanchez, J.C., Principe, J.C., Nishida, T., Bashirullah, R., Harris, J.G., Fortes, J.A.B.: Technology and Signal Processing for Brain-Machine Interfaces. *IEEE* 2, 29–40 (2008)
4. Chapin, J.K., Nicolelis, M.A.L.: Real-time control of a robot arm using simultaneously recorded neurons in the motor cortex. *Nature* 2(7) (1999)
5. Nicolelis, M.A.L., Chapin, J.K.: Controlling Robots with the Mind, pp. 46–53. *Scientific American* (2002)
6. Hochberg, L.R., Bacher, D., Jarosiewicz, B., Masse, N.Y.: Reach and grasp by people with tetraplegia using a neurally controlled robotic arm. *Nature* 485 (2012)
7. del R. Millan, J., Renkens, F., Mourino, J., Gerstner, W.: Non-Invasive Brain-Actuated Control of a Mobile Robot by Human EEG. *IEEE Trans. Biomed. Eng.* 51(6), 1026–1033 (2004)
8. Yamada, S.: Improvement and Evaluation of an EEG Keyboard Input Speed. *IEICE Technical Report*, pp. 329–336 (1996)
9. Qin, L., Ding, L., He, B.: Motor imagery classification by means of source analysis for brain-computer interface applications. *J. Neural Eng.* 1, 135–141 (2004)
10. McFarland, D.J., Miner, L.A., Vaughan, T.M., Wolpaw, J.R.: Mu and Beta Rhythm Topographies During Motor Imagery and Actual Movements. *Topography* 12(3), 177–186 (2000)
11. Dornhege, G., del R. Millan, J., Hinterger, T., McFarland, D.J., Muller, K.-R.: Toward Brain-Computer Interfacing. *Terrence J. Sejnowski*, 8–25 (2007)
12. Yanagida, H., Igasaki, T., Hayashida, Y., Murayama, N.: Analysis of corticomuscular wavelet coherence during isotonic contraction. *IEICE Technical Report*, pp. 25–28 (2007)
13. Grgic, S., Grigic, M., Zovko-Cihlar, B.: Performance Analysis of Image Compression Using Wavelet. *IEEE Transactions on Electronics* 48(3), 682–695 (2001)
14. Cole, M.O.T., Keogh, P.S., Burrows, C.R., Sahinkaya, M.N.: Adaptive Control of Rotor Vibration Using Compact Wavelets. *Journal of Vibration and Acoustics* 128, 653–665 (2006)
15. Kong, J., Shimada, H., Boyer, K., Saltz, J., Gurcan, M.: A New Multiresolution Analysis Framework for Classifying Grade of Neuroblastic Differentiation. *OSU BMI Technical Report:OSUBMI TR n02* (2007)
16. Addison, P.: *The Illustrated Wavelet Transform Handbook* (2002)